
Mixture Representation Learning with Coupled Autoencoders

Yeganeh M. Marghi¹ Rohan Gala¹ Uygr Sümbül¹

Abstract

Jointly identifying a mixture of discrete and continuous factors of variability without supervision is a key problem in unraveling complex phenomena. Variational inference has emerged as a promising method to learn interpretable mixture representations. However, posterior approximation in high-dimensional latent spaces, particularly for discrete factors remains challenging. Here, we propose an unsupervised variational framework using multiple interacting networks called *cpl-mixVAE* that scales well to high-dimensional discrete settings. In this framework, the mixture representation of each network is regularized by imposing a consensus constraint on the discrete factor. We justify the use of this framework by providing both theoretical and experimental results. Finally, we use the proposed method to jointly uncover discrete and continuous factors of variability describing gene expression in a single-cell transcriptomic dataset profiling more than a hundred cortical neuron types.

1. Introduction

Complex phenomena can be attributed to a mixture of discrete and continuous factors of variability. It is crucial to parse complexity in this manner for a variety of applications, from learning interpretable models for image generation, to quantifying factors of biological variability in single-cell studies. To this end, mixture modeling approaches propose to learn representations that jointly capture dependence of observations on discrete and continuous factors (Bengio et al., 2013).

Generative models for mixture modeling have recently received attention from the deep learning community. Deep Gaussian mixture models (Dilokthanakul et al., 2016; Johnson et al., 2016; Jiang et al., 2017) are among the first deep generative models for mixture modeling, in which a continuous representation is decomposed into discrete clusters.

However, such models focus on clustering without regard to interpretability. Various adversarial and variational methods have been proposed to learn interpretable continuous factors alongside: while existing adversarial generative models, e.g. InfoGAN (Chen et al., 2016), are susceptible to stability issues (Higgins et al., 2017; Kim & Mnih, 2018), variational autoencoders (VAEs) emerge as efficient and more stable alternatives (Tschannen et al., 2018; Zhang et al., 2018).

VAE-based approaches approximate the mixture model by assuming a family of distributions q_ϕ and select the member closest to the true model p . Popular choices in VAE implementations include (1) using KL divergence to compute discrepancy between q_ϕ and p , and (2) using a multivariate Gaussian mixture distribution with uniformly distributed discrete and isotropic Gaussian distributed continuous priors. However, such choices may lead to underestimating the posterior variance (Minka et al., 2005; Blei et al., 2017). Solutions to resolve this issue are mainly applicable in low-dimensional spaces or for continuous factors alone (Deasy et al., 2020; Kingma et al., 2016; Ranganath et al., 2016; Quiroz et al., 2018). Yet, the dimension of the latent space can be much larger in many application domains (e.g., cell biology, robotic systems, finance), and learning interpretable mixture representations remains challenging in practice, especially as model complexity increases. For instance, in the explosive field of single cell transcriptomics, hundreds of cell types are implicated as discrete variational factors of thousands of gene expression measurements.

Inspired by *collective decision making*, here we introduce a variational framework using multiple *autoencoding arms* to jointly infer interpretable finite discrete (categorical) and continuous factors in the presence of high-dimensional discrete space. Coupled-autoencoders have been previously studied in the context of multi-modal recordings, where each arm learns only a continuous latent representation for one of the data modalities (Feng et al., 2014; Gala et al., 2019; Lee & Pavlovic, 2020). However, it is not clear whether such architectures can be useful to study standalone (single modality) datasets: (i) Do they provide a fundamental advantage over a single arm? (ii) Does exploration via alignment across arms extend to discrete settings? We answer both of these questions in the affirmative by using pairwise-coupled autoencoders for a single data modality that imposes a consensus constraint on the posterior, in an

¹Allen Institute, WA, USA. Correspondence to: Yeganeh M. Marghi <yeganeh.marghi@alleninstitute.org>.

unsupervised fashion. We demonstrate that by acknowledging the dependencies of continuous and categorical factors and exploiting category-dependent variabilities, the coupled multi-arm architecture enhances accuracy, robustness, and interpretability of the inferred factors without requiring any prior on the relative abundances of categories.

Our contributions can be summarized as follows: (i) We theoretically justify the advantage of the multi-arm VAE framework as a collective decision maker for more accurate inference. (ii) We formulate collective decision making as a variational inference problem with multiple VAE arms and show that this formulation is equivalent to a collection of constrained VAEs. The proposed constraint is defined based on the Aitchison geometry in the simplex, which avoids mode collapse. (iii) We benchmark our method and demonstrate its superiority over comparable approaches using multiple datasets including a single cell gene expression dataset, described by an unstructured data matrix of $\sim 20,000$ neurons by 5,000 genes. We demonstrate that our method can be used to discover neuronal types as discrete categories and type-specific genes regulating the continuous within-type variability, such as metabolic state or disease state.

Related work. There is an extensive body of research on clustering in mixture models (Dilokthanakul et al., 2016; Jiang et al., 2017; Tian et al., 2017; Guo et al., 2016; Locatello et al., 2018b). The idea of improving the clustering performance through seeking a consensus and co-training across multiple observations has been explored in both unsupervised (Monti et al., 2003; Kumar & Daumé, 2011) and semi-supervised contexts (Blum & Mitchell, 1998). However, these methods do not consider the underlying continuous variabilities across observations. Beyond assigning clusters, in our framework, autoencoding arms seek a consensus at the time of learning mixture representations.

The proposed framework does not need supervision since the individual arms provide a form of prior or weak supervision for each other. In this regard, our paper is related to a body of work that attempts to improve representation learning by using semi-supervised or group-based settings (Bouchacourt et al., 2017; Hosoya, 2019; Nemeth, 2020). Bouchacourt et al. (2017) demonstrated a multi-level variational autoencoder (MLVAE) as a semi-supervised VAE by revealing that observations within groups share the same type. Hosoya (2019) and Nemeth (2020) attempted to improve MLVAE by imposing a weaker condition to the grouped data. In recent studies (Shu et al., 2019; Locatello et al., 2020), a weakly supervised variational setting has been proposed for disentangled representation learning by providing pairs of observations that share at least one underlying factor. They all rely on learning latent variables in continuous spaces, and have been only applied to image datasets with low-dimensional latent space.

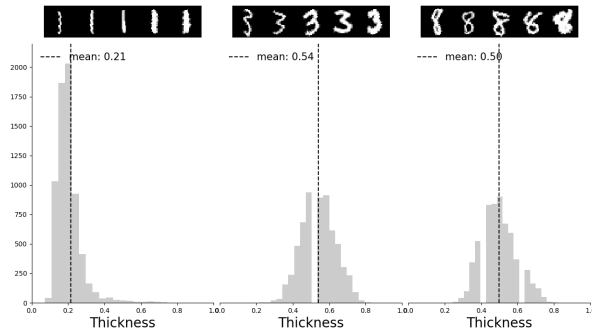


Figure 1. Empirical distributions for the continuous state variable representing stroke width are digit-dependent, illustrating dependence of style (width) on type (digit).

Recent advances in structured variational methods, such as imposing a prior (Ranganath et al., 2016) or spatio-temporal dependencies (Quiroz et al., 2018) on the latent distribution parameters, allows for scaling to larger dimensions. However, these solutions are not directly applicable to the discrete space, which will be addressed in our A-arm VAE framework.

2. Single mixture VAE framework

For an observation $\mathbf{x} \in \mathbb{R}^D$, a VAE learns a generative model $p_\theta(\mathbf{x}|\mathbf{z})$ and a variational distribution $q_\phi(\mathbf{z}|\mathbf{x})$, where $\mathbf{z} \in \mathbb{R}^M$ for $M \ll D$ is a latent variable with a parameterized distribution $p(\mathbf{z})$ (Kingma & Welling, 2013). *Disentangling* different sources of variability into different dimensions of \mathbf{z} enables an interpretable selection of latent factors (Higgins et al., 2017; Locatello et al., 2018a). However, in many real-world applications, the inherent mixture distribution of continuous and discrete variations is often overlooked. This problem can be addressed within the VAE framework in an unsupervised fashion by introducing a categorical latent variable $\mathbf{c} \in \mathcal{S}^K$, denoting the class label defined in a K -simplex, alongside the continuous latent variable $\mathbf{s} \in \mathbb{R}^M$. Here, we refer to the continuous variable \mathbf{s} as the *state* or *style* variable interchangeably. Assuming \mathbf{s} and \mathbf{c} are independent random variables, the evidence lower bound (ELBO) (Blei et al., 2017) for a single mixture VAE with the distributions parameterized by θ and ϕ is given by,

$$\mathcal{L}(\phi, \theta) = \mathbb{E}_{q_\phi(\mathbf{s}, \mathbf{c}|\mathbf{x})} [\log p_\theta(\mathbf{x}|\mathbf{s}, \mathbf{c})] - D_{KL}(q_\phi(\mathbf{s}|\mathbf{x})\|p(\mathbf{s})) - D_{KL}(q_\phi(\mathbf{c}|\mathbf{x})\|p(\mathbf{c})) \quad (1)$$

Maximizing ELBO in Eq. 1 imposes characteristics on $q(\mathbf{s}|\mathbf{x})$ and $q(\mathbf{c}|\mathbf{x})$ that can result in underestimation of posterior probabilities such as the mode collapse problem, where the network ignores a subset of latent variables (Minka et al., 2005; Blei et al., 2017). Recently, VAE-based solutions were proposed by imposing a uniform structure on $p(\mathbf{c})$: akin to β -VAE (Higgins et al., 2017; Burgess et al., 2018), JointVAE (Dupont, 2018) modified

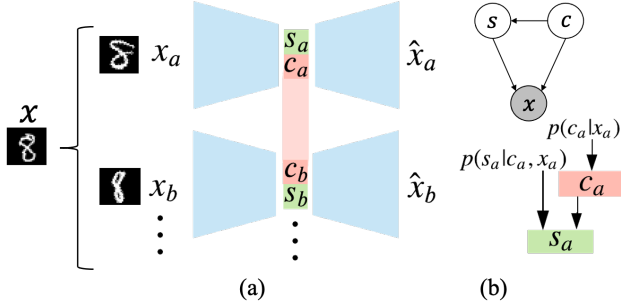


Figure 2. (a) Multi-arm autoencoder framework proposed as cplmixVAE model. Individual arms receive non-identical noisy copies of given samples \mathbf{x} , i.e. $\{\mathbf{x}_a, \mathbf{x}_b, \dots\}$, where they all belong to the same category, to learn mixture representations, i.e. $\{q(\mathbf{c}_a, \mathbf{s}_a), q(\mathbf{c}_b, \mathbf{s}_b), \dots\}$. VAE arms cooperate to learn the categorical assignment, $p(\mathbf{c})$. Cooperation is achieved by imposing a penalty on mismatches in the categorical assignments. (b) Each autoencoder learns type dependence of the state variable according to the graphical model.

the ELBO by assigning a pair of controlled information capacities for each variational factor, i.e. $\mathcal{C}_s \in \mathbb{R}^{|\mathbf{s}|}$ and $\mathcal{C}_c \in \mathbb{R}^{|\mathbf{c}|}$. The main drawback of JointVAE is that its performance is tied to heuristic tuning of $|\mathbf{s}| \times |\mathbf{c}|$ capacities over training iterations, which is not easily scalable to high-dimensional settings. CascadeVAE (Jeong & Song, 2019) suggested another VAE-based mixture model that maximizes the ELBO through a semi-gradient-based algorithm by iterating over two separate optimizations for the continuous and categorical variables. Although the computational cost for the additional optimization for the categorical variable has an approximately linear dependence on the number of categories and batch size, it can still be a deterrent for problems with numerous categories and unbalanced datasets requiring larger batch sizes. Thus, earlier solutions fall short of efficiently learning interpretable mixture representations for high-dimensional discrete spaces.

In addition to the issues discussed above, the performance and interpretability of those approaches are further limited by the common assumption that the continuous variable representing the style of the data is independent of the categorical variable. In practice, style often depends on the class label. For instance, even for the well-studied MNIST dataset, the histograms of common digit styles, e.g. “width”, markedly vary for different digits (Fig. 1). Moreover, further analysis of the identified continuous factor in the earlier approaches reveals that the independence assumption among $q(\mathbf{s}|\mathbf{x})$ and $q(\mathbf{c}|\mathbf{x})$ can be significantly violated (see Supplementary G and H).

3. Coupled mixture VAE framework

The key intuition behind multi-arm networks is cooperation for decision making to improve posterior estimation. Collective decision making has been studied under different contexts and a popular name referring to its advantages is the

“wisdom of the crowd” (Surowiecki, 2005). When unanimous decisions made by a crowd (multiple arms) form a probability distribution, multiple estimates from the same sample increase the expected probability of a true assignment.

A-arm VAE Framework. We define the A -arm VAE as an A -tuple of independent and architecturally identical autoencoding arms, where the a -th arm parameterizes a mixture model distribution (Fig. 2a). In this framework, individual arms receive a collection of non-identical copies, i.e. $\{\mathbf{x}_a, \mathbf{x}_b, \dots\}$ of the given sample, i.e. \mathbf{x} , with the same class label. While each arm has its own mixture representation with potentially non-identical parameters, all arms cooperate to learn $q(\mathbf{c}_a|\mathbf{x}_a)$ via a cost function at the time of training. Accordingly, a crowd of VAEs with A arms can be formulated as a collection of constrained variational objectives as follows.

$$\max \quad \mathcal{L}_{\mathbf{s}_1|\mathbf{c}_1}(\phi_1, \theta_1) + \dots + \mathcal{L}_{\mathbf{s}_A|\mathbf{c}_A}(\phi_A, \theta_A) \quad (2)$$

$$\text{s.t. } \mathbf{c}_1 = \dots = \mathbf{c}_A$$

where $\mathcal{L}_{\mathbf{s}_a|\mathbf{c}_a}(\phi_a, \theta_a)$ is the variational loss for arm a ,

$$\begin{aligned} \mathcal{L}_{\mathbf{s}_a|\mathbf{c}_a}(\phi_a, \theta_a) = & \mathbb{E}_{q(\mathbf{s}_a, \mathbf{c}_a|\mathbf{x}_a)} [\log p(\mathbf{x}_a|\mathbf{s}_a, \mathbf{c}_a)] \\ & - \mathbb{E}_{q(\mathbf{c}_a|\mathbf{x}_a)} [D_{KL}(q(\mathbf{s}_a|\mathbf{c}_a, \mathbf{x}_a) \| p(\mathbf{s}_a|\mathbf{c}_a))] \\ & - \mathbb{E}_{q(\mathbf{s}_a|\mathbf{c}_a, \mathbf{x}_a)} [D_{KL}(q(\mathbf{c}_a|\mathbf{x}_a) \| p(\mathbf{c}_a))]. \end{aligned} \quad (3)$$

In Eq. (3), the variational loss for each arm is defined according to the graphical model in Fig. 2b, which is built upon the traditional ELBO in Eq. (1) by conditioning the continuous state on the categorical variable (derivation in Supplementary Section B).

Arms observe non-identical copies of samples. In the A -arm VAE framework, VAE arms receive non-identical observations that share the discrete variational factor. To achieve this in a fully unsupervised setting, we use *type-preserving* data augmentation that generates independent and identically distributed copies of data while preserving its categorical identity. For image datasets, conventional transformations such as rotation, scaling, or translation can serve as type-preserving augmentations. However, for non-image datasets, e.g. single-cell data, we seek a generative model that learns transformations representing within-class variability in an unsupervised manner. To this end, inspired by DAGAN (Antoniou et al., 2017) and VAE-GAN (Larsen et al., 2016), we develop a generative model to provide collections of observations for our multi-arm framework (for additional information, see supplementary Section F).

In Supplementary Section A, Remark 2, we further discuss an under-exploration scenario in data augmentation, in which the augmented samples are not independently distributed and are concentrated around the given sample.

The consensus constraint in the A -arm framework (Eq. 2) regularizes the posterior approximation and enhances varia-

tional inference accuracy compared to a single VAE. This is theoretically justified by Propositions 1 and 2.

Definition 1. (Confidence) Suppose \mathbf{x} is generated by a multivariate mixture distribution so that $p(\mathbf{x}) = \sum_c \int_s p(\mathbf{x}|s, c)p(s|c)p(c) ds$, where $p(c)$ and $p(s|c)$ denote arbitrary distributions for discrete and continuous factors, respectively. For samples belonging to category “ m ”, the assignment confidence for category “ k ” can be expressed as,

$$\mathcal{C}_m(k) = \mathbb{E}_{\mathbf{x}|m} [\log p(c = k|\mathbf{x})]. \quad (4)$$

Consequently, $\mathcal{C}_m(m)$ denotes the confidence of the mixture model for the true categorical factor. In the following propositions, we use $\mathcal{C}_m^A(\cdot)$ to convey the categorical confidence of the A -arm framework, where $A > 0$ denotes the number of VAE arms.

Proposition 1. Consider the problem of mixture representation learning in a multi-arm VAE framework. For $A > B \geq 1$ and $\forall m$,

$$\mathcal{C}_m^A(m) > \mathcal{C}_m^B(m). \quad (5)$$

(Proof in Supplementary Section A)

Proposition 2. In the A -arm VAE framework, there exists an A such that $\forall m, n, m \neq n$,

$$\mathcal{C}_m^A(m) > \mathcal{C}_m^A(n), \quad (6)$$

independent of the relative abundances of categories. (Proof in Supplementary Section A)

Thus, the consensus constraint is sufficient to enhance inference for mixture representations in the A -arm VAE framework. Our theoretical results show that the minimum number of arms guaranteeing correct assignment is a function of the prior distribution for the categorical variable and category-dependent distribution. While in an unsupervised approach, defining the required number of arms in the absence of the categorical prior and category-dependent information remains a challenge, we now show that in the particular case of uniformly distributed categories, one pair of coupled arms is enough to satisfy Eq. 6.

Corollary 1. For a uniform prior on the discrete factor, one pair of VAE arms ($A = 2$) is sufficient to satisfy Eq. 6. (see Supplementary Section A)

We emphasize the joint presence of discrete and continuous factors in these results. Unlike Bouchacourt et al. (2017); Shu et al. (2019); Locatello et al. (2020), the suggested framework is not restricted to the continuous space, and does not require any weak supervision as (Bouchacourt et al., 2017). Instead, it relies on representations that are invariant under non-identical copies of observations.

3.1. cpl-mixVAE: pairwise coupling in A -arm VAE

In the A -arm VAE framework, the mixture representation is obtained through the optimization in Eq. 2. Not only is it challenging to solve the maximization in Eq. 2 due to the equality constraint, but the objective remains a function of $p(c)$ which is unknown, and typically non-uniform. To overcome this, we use an equivalent formulation for Eq. 2 by applying the pairwise coupling paradigm as follows (details of derivation in Supplementary Section C).

$$\begin{aligned} \max \quad & \sum_{a=1}^A (A-1) \left(\mathbb{E}_{q(\mathbf{s}_a, \mathbf{c}_a | \mathbf{x}_a)} [\log p(\mathbf{x}_a | \mathbf{s}_a, \mathbf{c}_a)] - \right. \\ & \left. \mathbb{E}_{q(\mathbf{c}_a | \mathbf{x}_a)} [D_{KL}(q(\mathbf{s}_a | \mathbf{c}_a, \mathbf{x}_a) \| p(\mathbf{s}_a | \mathbf{c}_a))] \right) - \\ & \sum_{a < b} \mathbb{E}_{q(\mathbf{s}_a | \mathbf{c}_a, \mathbf{x}_a)} \mathbb{E}_{q(\mathbf{s}_b | \mathbf{c}_b, \mathbf{x}_b)} [\mathcal{D}(a, b)] \\ \text{s.t.} \quad & \mathbf{c}_a = \mathbf{c}_b \quad \forall a, b \in [1, A], a < b \end{aligned} \quad (7)$$

where $\mathcal{D}(a, b) = D_{KL}(q(\mathbf{c}_a | \mathbf{x}_a)q(\mathbf{c}_b | \mathbf{x}_b) \| p(\mathbf{c}_a, \mathbf{c}_b))$, is the KL divergence across coupled arms, which is a function of the joint distribution $p(\mathbf{c}_a, \mathbf{c}_b)$, rather than $p(c)$.

We relax the optimization in Eq. 7 into an unconstrained problem by marginalizing the joint distribution over a mismatch measure between categorical variables (full derivation in Supplementary Section D).

$$\begin{aligned} \max \quad & \sum_{a=1}^A (A-1) \left(\mathbb{E}_{q(\mathbf{s}_a, \mathbf{c}_a | \mathbf{x}_a)} [\log p(\mathbf{x}_a | \mathbf{s}_a, \mathbf{c}_a)] - \right. \\ & \left. \mathbb{E}_{q(\mathbf{c}_a | \mathbf{x}_a)} [D_{KL}(q(\mathbf{s}_a | \mathbf{c}_a, \mathbf{x}_a) \| p(\mathbf{s}_a | \mathbf{c}_a))] \right) + \\ & \sum_{a < b} H(\mathbf{c}_a | \mathbf{x}_a) + H(\mathbf{c}_b | \mathbf{x}_b) - \lambda \mathbb{E}_{q(\mathbf{c}_a, \mathbf{c}_b | \mathbf{x}_a, \mathbf{x}_b)} [d^2(\mathbf{c}_a, \mathbf{c}_b)] \end{aligned} \quad (8)$$

In Eq. 8, in addition to entropy-based confidence penalties known as mode collapse regularizers (Pereyra et al., 2017), the distance measure $d(\mathbf{c}_a, \mathbf{c}_b)$ encourages a consensus on the categorical assignment controlled by $\lambda \geq 0$, called *coupling* hyperparameter.

We refer to the model in Eq. 8 as *cpl-mixVAE* (Fig. 2a). In *cpl-mixVAE*, VAE arms try to achieve identical categorical assignments while independently learning their own style variables. Here, we set $\lambda = 1$ universally, though further optimization is possible. While the bottleneck architecture already encourages interpretable continuous variables, this formulation can be easily extended to include an additional hyperparameter to promote disentanglement of continuous variables as in β -VAE (Higgins et al., 2017).

It is also instructive to cast Eq. 8 in an equivalent constrained variational optimization.

Remark 1. The A -arm VAE framework is a collection of

constrained variational models as follows,

$$\begin{aligned} \max \quad & \sum_{a=1}^A \mathbb{E}_{q(\mathbf{s}_a, \mathbf{c}_a | \mathbf{x}_a)} [\log p(\mathbf{x}_a | \mathbf{s}_a, \mathbf{c}_a)] - \\ & \mathbb{E}_{q(\mathbf{c}_a | \mathbf{x}_a)} [D_{KL}(q(\mathbf{s}_a | \mathbf{c}_a, \mathbf{x}_a) \| p(\mathbf{s}_a | \mathbf{c}_a))] + H(\mathbf{c}_a | \mathbf{x}_a) \\ \text{s.t.} \quad & \mathbb{E}_{q(\mathbf{c}_a | \mathbf{x}_a)} [d^2(\mathbf{c}_a, \mathbf{c}_b)] < \epsilon \end{aligned} \quad (9)$$

where ϵ denotes the strength of the consensus constraint. Here, \mathbf{c}_b indicates the assigned category by any one of the arms, $b \in \{1, \dots, A\}$, imposing structure on the discrete variable as an approximation of the prior.

Distance between categorical variables. $d(\mathbf{c}_a, \mathbf{c}_b)$ denotes the distance between a pair of $|\mathbf{c}|$ -dimensional unordered categorical variables, which are associated with probability vectors with non-negative entries and sum-to-one constraint that form a K -dimensional simplex, where $K = |\mathbf{c}|$. In the real space, a typical choice to compute the distance between two vectors is using Euclidean geometry. However, this geometry is not suitable for probability vectors. Here, we utilize *Aitchison geometry* (Aitchison, 1982; Egozcue et al., 2003), which defines a substitute vector space on the simplex. Accordingly, the distance in the simplex, i.e. $d_{S^K}(\mathbf{c}_a, \mathbf{c}_b)$ is defined as $d_{S^K}(\mathbf{c}_a, \mathbf{c}_b) = \|\text{clr}(\mathbf{c}_a) - \text{clr}(\mathbf{c}_b)\|_2, \forall \mathbf{c}_a, \mathbf{c}_b \in S^K$, where $\text{clr}(\cdot)$ denotes the *isometric centered-log-ratio* transformation in the simplex. This categorical distance satisfies the conditions of a mathematical metric according to Aitchison geometry.

3.2. Handshake in the simplex

An instance of the well-known mode collapse problem (Lucas et al., 2019) manifests itself in the minimization of $d_{S^K}(\mathbf{c}_a, \mathbf{c}_b)$ (Eq. 8): its trivial local optima encourages the network to abuse the discrete latent factor by ignoring many of the available categories. For instance, in an extreme case, the network learns $\mathbf{c}_a = \mathbf{c}_b = \mathbf{c}_0$. In this scenario, the continuous variable is compelled to act as a primary latent factor, while the model fails to deliver an interpretable mixture representation despite achieving an overall low loss value.

To avoid such undesirable local equilibria while training, we add perturbations to the categorical representation of each arm, where the perturbation of each arm, i.e. $\mathbf{p}_a \in S^K$ is a function of mini-batch statistics. If posterior probabilities in the simplex have a small dispersion, the perturbed distance calculation overstates the discrepancies. Instead of minimizing $d_{S^K}^2(\mathbf{c}_a, \mathbf{c}_b)$, we minimize a perturbed distance $d_\sigma^2(\mathbf{c}_a, \mathbf{c}_b) = \sum_k (\sigma_{a_k}^{-1} \log c_{a_k} - \sigma_{b_k}^{-1} \log c_{b_k})^2$, where $\sigma_{a_k}^2$ and $\sigma_{b_k}^2$ indicate the mini-batch variance of the k -th category, for arms a and b . We show that the perturbed distance $d_\sigma(\cdot)$ is bounded by $d_{S^K}(\cdot)$ and non-negative values ρ_u, ρ_l , which are function of $d_{S^K}(\mathbf{p}_a, \mathbf{p}_b)$.

Proposition 3. Suppose $\mathbf{c}_a, \mathbf{c}_b \in S^K$, where S^K is a simplex of $K > 0$ parts. If $d_{S^K}(\mathbf{c}_a, \mathbf{c}_b)$ denotes the distance in Aitchison geometry and $d_\sigma^2(\mathbf{c}_a, \mathbf{c}_b) = \sum_k (\sigma_{a_k}^{-1} \log c_{a_k} - \sigma_{b_k}^{-1} \log c_{b_k})^2$ denotes a perturbed distance, then

$$d_{S^K}^2(\mathbf{c}_a, \mathbf{c}_b) - \rho_l \leq d_\sigma^2(\mathbf{c}_a, \mathbf{c}_b) \leq d_{S^K}^2(\mathbf{c}_a, \mathbf{c}_b) + \rho_u$$

where $\rho_u, \rho_l \geq 0$, $\rho_u = K(\tau_{\sigma_u}^2 + \tau_c^2) + 2\Delta_\sigma \tau_c$, $\rho_l = \frac{\Delta_\sigma^2}{K} - K\tau_{\sigma_l}^2$, $\tau_c = \max_k \{\log c_{a_k} - \log c_{b_k}\}$, $\tau_{\sigma_u} = \max_k \{g_k\}$, $\tau_{\sigma_l} = \max_k \{-g_k\}$, $\Delta_\sigma = \sum_k g_k$, and $g_k = (\sigma_{a_k}^{-1} - 1) \log c_{a_k} - (\sigma_{b_k}^{-1} - 1) \log c_{b_k}$. (Proof in Supplementary Section E)

Thus, when \mathbf{c}_a and \mathbf{c}_b are similar and their spread is not small, $d_\sigma(\mathbf{c}_a, \mathbf{c}_b)$ closely approximates $d_{S^K}(\mathbf{c}_a, \mathbf{c}_b)$. Otherwise, it diverges from $d_{S^K}(\cdot)$ to avoid mode collapse.

4. Experiments

We used three datasets: MNIST, dSprites, and a single-cell RNA-sequencing dataset (scRNA-seq) (Tasic et al., 2018). For the scRNA-seq dataset, identifying interpretable biological variables is a challenge: neuronal cells, the basic building blocks of the brain, display both significant diversity and stereotypy in their gene expression. Individual cells can differ due to either their *type* or continuous *within-type* variations (Trapnell, 2015; Andrews & Hemberg, 2018), which are considered as biological interpretations of discrete and continuous variabilities. Identifying such factors can be useful to study canonical brain circuits in terms of their *generic* components (Bargmann et al., 2014), and to identify gene expression programs (Trapnell, 2015), both of which are high-priority research areas in neuroscience.

Although MNIST and dSprites datasets do not require high-dimensional settings for mixture representation, to facilitate comparisons of cpl-mixVAE with earlier methods, first we report the results for these benchmark datasets.

We trained three unsupervised VAE-based methods for mixture modeling: JointVAE (Dupont, 2018), CascadeVAE (Jeong & Song, 2019), and ours (cpl-mixVAE). For MNIST, we additionally trained the popular InfoGAN (Chen et al., 2016) as the most comparable GAN-based model. To report the interpretability of the mixture representations, we consider the accuracy (ACC) of categorical assignments for the discrete variable and latent traversal analysis for the continuous variable by fixing the discrete factor and changing the continuous variable according to $p(\mathbf{s} | \mathbf{c}, \mathbf{x})$. Additionally, we report the computational efficiency (number of iterations per second) to compare the training complexity of the multi-arm framework against earlier methods (Table 1). All reported numbers for cpl-mixVAE models are average accuracies calculated across arms.

Table 1. Training results for 10 randomly initialized runs. cpl-mixVAE uses 2 arms. $|c|$ and $|s|$ denote the cardinality of latent discrete and continuous spaces. Chance-level indicates the chance level of classification accuracy for each dataset. ACC denotes the accuracy of the categorical assignment. Computation denotes the training speed (iteration/second) on a GeForce RTX 2080 Ti GPU. The computation of cpl-mixVAE includes the entire execution time for training one pair of coupled networks, plus data augmentation.

Dataset	Chance-level	$ c $	$ s $	Method	ACC (%) \uparrow (mean \pm s.d.)	Computation \uparrow (iteration/sec)	Disentanglement score
MNIST	10.0%	10	2	InfoGAN	77.87 \pm 21.68	12.2	-
			10	JointVAE	68.99 \pm 11.76	74.1	
				CascadeVAE	81.41 \pm 09.54	23.8	
				cpl-mixVAE	84.56 \pm 06.47	17.5	
dSprite	33.3%	3	6	JointVAE	44.79 \pm 03.88	52.6	74.51 \pm 05.17
			CascadeVAE	78.84 \pm 15.65	15.4	90.49 \pm 05.28	
			cpl-mixVAE	96.30 \pm 09.15	20.6	89.98 \pm 04.09	
scRNA-seq	06.3%	115	2	JointVAE	12.53 \pm 01.83	28.6	-
			CascadeVAE	02.69 \pm 00.05	03.4		
			cpl-mixVAE	38.78 \pm 01.26	10.1		

During training of VAE-based models, to sample from $q(\mathbf{c}_a | \mathbf{x}_a)$, we use the Gumbel-softmax distribution (Jang et al., 2016; Maddison et al., 2014) with a temperature parameter $0 < \tau \leq 1$. In cpl-mixVAE, each arm received an augmented copy of the original input generated by the deep generative augmenter (Supplementary Section F), while training. Details of the networks architectures and training settings can be found in Supplementary Section J.

4.1. Benchmark datasets

MNIST. Based on the uniform distribution of handwritten digits in MNIST, we used a 2-arm cpl-mixVAE to learn interpretable representations. Following the convention (Chen et al., 2016; Dupont, 2018; Jeong & Song, 2019), each arm of cpl-mixVAE uses a 10-dimensional categorical variable representing digits (type), and a 10-dimensional continuous random variable representing the writing style (state). Table 1 displays the classification performance of the discrete latent variable (the predicted class label) for InfoGAN, two 1-arm VAE methods (JointVAE and CascadeVAE), and cpl-mixVAE with 2 arms. Additionally, Fig. 3 (top panel) illustrates the continuous latent traversals for four dimensions of the state variable inferred by cpl-mixVAE, where each row corresponds to a different dimension of the categorical variable, and the state variable monotonically changes across columns. Both results in Table 1 and Fig. 3 show that cpl-mixVAE achieved an interpretable mixture representation with the highest categorical assignment accuracy.

dSprites. Similarly, due to the uniform distribution of classes, we again used a 2-arm cpl-mixVAE model. Results in Table 1 verifies that our method outperforms the other methods in terms of categorical assignment accuracy. To report the intractability of the continuous variable, in addition to demonstrating the traversal results (Fig. 3 (bottom panel)), we reported disentanglement scores. For a fair comparison, we used the same disentanglement metric implemented for CascadeVAE (Jeong & Song, 2019).

Summary. cpl-mixVAE improves the accuracy of categorical assignments and infers better mixture representations. It outperforms earlier methods, without using extraneous optimization or heuristic channel capacities. Beyond performance and robustness, its computational cost is also comparable to that of the baselines.

4.2. scRNA-seq

scRNA-seq datasets are significantly more complex than a typical machine learning dataset. Here, the scRNA-seq dataset includes transcriptomic profiles of 10,000 genes for 22,365 cells, from over 100 cell types with sizeable differences between the relative abundances of clusters. Hence, two main challenges of representation learning in this dataset are (i) large number of cell types (discrete variable), and (ii) class imbalance – the most- and the least-abundant cell types include 1404 and 16 samples, respectively. Moreover, whether the observed diversity corresponds to discrete variability or a continuum is an ongoing debate in neuroscience. While using genes that are differentially expressed in subsets of cells, known as *marker genes* (MGs) (Trapnell, 2015) is a common approach to define cell types, the identified genes rarely obey the idealized MG definition in practice. Identifying these biomarkers is a challenging process, since highest variance genes are often expressed and may be known markers for multiple cell types. Here, we focus on *neuronal* cells and use a subset of 5,000 highest variance genes. The original neuroscience study suggested 115 discrete neuronal types, based on an MG-based approach (Tasic et al., 2018).

Neuron type identification. We trained mixture VAE-based models using 115- and 2-dimensional discrete and continuous variables. We compared the suggested cell types in (Tasic et al., 2018) with the discrete representations that are inferred from VAE models. Table 1 and Fig. 4 demonstrate the performance of a 2-arm cpl-mixVAE model against JointVAE and CascadeVAE. Our results clearly show that cpl-mixVAE outperforms JointVAE and CascadeVAE

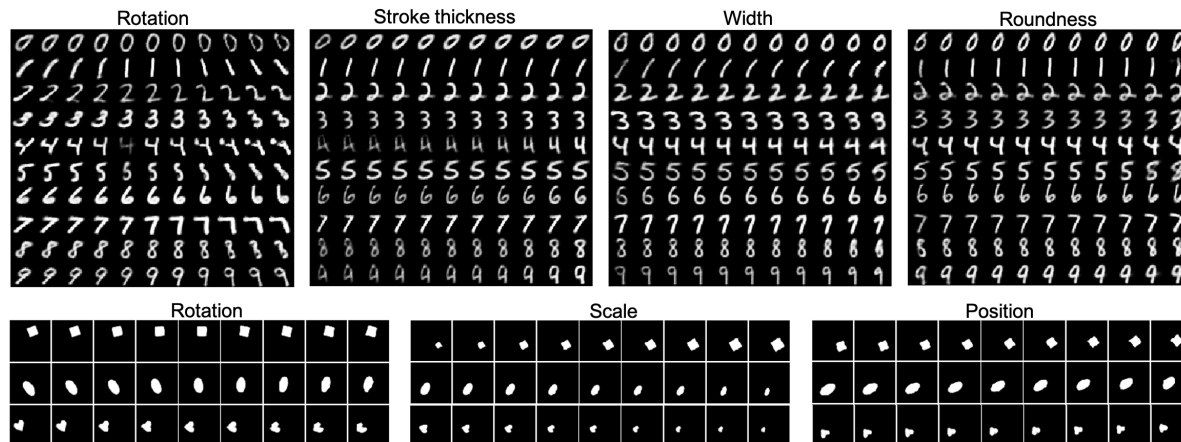


Figure 3. Interpretable continuous latent traversals of 1-st arm of the cpl-mixVAE framework with two autoencoders, for MNIST (top panel) and dSprites (bottom panel). The discrete variable c is constant for all reconstructions in the same row.

in identifying meaningful known cell types.

Using $A > 2$. Unlike the discussed benchmark datasets, the neuronal types are not uniformly distributed. Accordingly, we also investigated the accuracy improvement for categorical assignment when more than two arms are used. Fig. 5 illustrates the accuracy improvement with respect to a single autoencoder model, i.e. JointVAE, in agreement with our theoretical findings.

Identifying genes regulating cell activity. To examine the role of the continuous latent variable, we applied a similar traversal analysis to that used for the benchmark datasets. For a given cell sample and its discrete type, we changed each dimension of the continuous variable using the conditional distribution, and inspected gene expression changes caused by continuous variable alterations. Fig. 6 shows the results of the continuous traversal study for a 1-arm VAE (JointVAE) and a 2-arm VAE (cpl-mixVAE), for two excitatory neurons belonging to the “L5 NP” (cell type (I)) and “L6 CT” (cell type (II)) sub-classes. In each sub-figure, the latent traversal is color-mapped to normalized reconstructed expression values, where the y -axis corresponds to one dimension of the continuous variable, and the x -axis corresponds to three gene subsets, namely (i) MGs for the two excitatory types, (ii) immediate early genes (IEGs), and (iii) housekeeping gene (HKGs) subgroups (Hrvatin et al., 2018; Tarasenko et al., 2017). For cpl-mixVAE (Fig. 6b), the normalized expression of the reported MGs as indicators for excitatory cell types (discrete factors) is unaffected by changes of identified continuous variables. In contrast, for JointVAE (Fig. 6a), we observed that the normalized expression of some MGs (5 out of 10) are changed due to the continuous factor traversal. Additionally, we found that the expression changes inferred by cpl-mixVAE for IEGs and HKGs are essentially *monotonically* linked to the continuous variable, confirming that the expression of

IEGs and HKGs depends strongly on the cell activity variations under different metabolic and environmental conditions. Conversely, JointVAE fails to reveal such activity-regulated monotonicity for IEGs and HKGs. Furthermore, our results for cpl-mixVAE reveal that the expression of activity-regulated genes depends on the cell type, i.e. IEGs and HKGs respond differently to activation depending on their cell types (compare rows I and II in Fig. 6b). However, in Fig. 6a, since the baseline 1-arm VAE does not take into account the dependency of discrete and continuous factors, it fails to reveal the dependence of activity-regulated expression to the cell type, and therefore produces identical expressions for both types (I) and (II).

Summary. While both JointVAE and CascadeVAE failed to identify cell types as discrete factors, cpl-mixVAE successfully identified the majority of known types. Our findings suggest that cpl-mixVAE by acknowledging the dependencies of continuous and categorical factors, captures relevant and interpretable continuous variability that can provide insight when deciphering the molecular mechanisms shaping the landscape of biological states, e.g. metabolic or disease.

4.3. Ablation studies

To elucidate the success of the A-arm VAE framework in mixture modeling, we investigate the categorical assignment performance under different training settings. Since CascadeVAE does not learn the categorical factors by variational inference, here we mainly study JointVAE (as a 1-arm VAE) and cpl-mixVAE (as a 2-arm VAE). First, to isolate the impact of data augmentation in training, we trained JointVAE[†], where the JointVAE model was trained with noisy copies of the original MNIST dataset, same as cpl-mixVAE. The results in Table S1 (see Supplementary Section I) for JointVAE[†] suggest that data augmentation by itself does not enhance the categorical assignment. Sub-

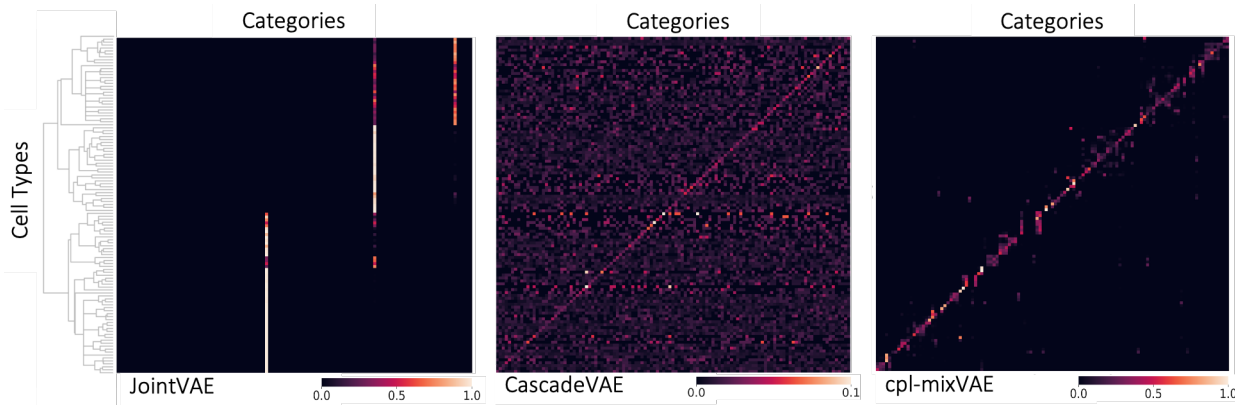


Figure 4. Categorical assignments for the scRNA-seq dataset. Confusion matrices of JointVAE, CascadeVAE, and cpl-mixVAE trained by $|c| = 115$, $|s| = 2$. The dendrogram on the y-axis shows MG-based hierarchical classification with 115 cell types, suggested by Tasic et al., 2018. Implementation details for each model can be found in Supplementary Section J.

sequently, to understand whether architectural differences put JointVAE at a disadvantage, we trained JointVAE[‡] (Table S1), which uses the same architecture as the one used in cpl-mixVAE. JointVAE[‡] uses the same learning procedure as JointVAE, but its convolutional layers are replaced by fully-connected layers (see Supplementary Section I and J for details). The result for JointVAE[‡] suggests that the superiority of cpl-mixVAE is not due to the network architecture either. Furthermore, we examined the performance changes of the proposed 2-arm cpl-mixVAE under three different settings: (i) cpl-mixVAE*, where coupled networks are not independent and network parameters are shared; (ii) cpl-mixVAE^a, where only random rotations ($[-\pi/9, \pi/9]$) are used as an affine transformation for data augmentation; and (iii) cpl-mixVAE($s \not\parallel c$), where the state variable is independent of the discrete variable (Table S1). Our results show that the proposed cpl-mixVAE obtained the best categorical assignments across all training settings.

Summary. We experimentally observe that inference does not improve in 1-arm VAEs by using either augmented copies or cpl-mixVAE’s single network design. Additionally, when within-class variations can be guessed (image datasets), using a simple augmentation strategy, e.g. cpl-mixVAE^a, is sufficient for the A-arm VAE framework.

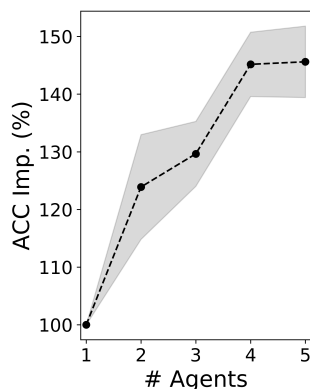


Figure 5. Improvement of the categorical representation (ACC) of cpl-mixVAE by adding more agents to the multi-arm framework. A-arm’s performance for $A \geq 2$ is compared with the baseline 1-arm, JointVAE. The reported results belong to 3 randomly initialized runs.

5. Conclusion

We have proposed cpl-mixVAE as a multi-arm framework to apply the power of collective decision making in unsupervised joint representation learning of discrete and continuous factors, scalable to the high-dimensional discrete space. This framework utilizes multiple pairwise-coupled autoencoding arms with a shared categorical variable, while independently learning the continuous variables. Our experimental results for all three datasets support the theoretical findings, and show that cpl-mixVAE outperforms comparable models. Importantly, for a challenging scRNA-seq dataset, we showed that the proposed framework can identify biologically interpretable cell types and differentiate between type-dependent and activity-regulated genes.

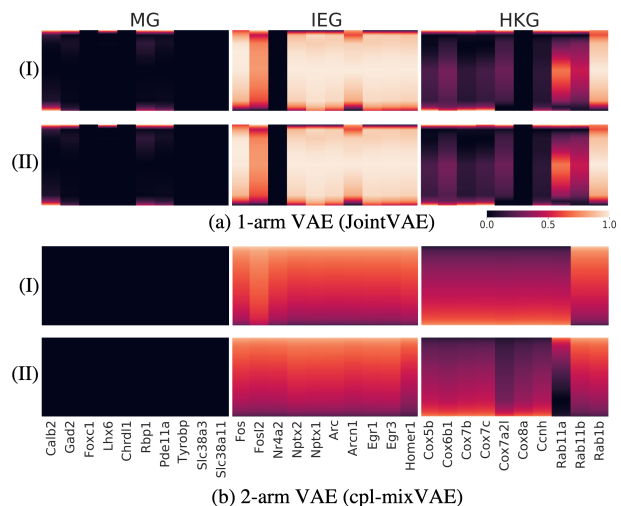


Figure 6. Continuous latent traversal analysis for two excitatory cell types (I “L5 NP ALM Trhr Nefl” and II “L6 CT Nxph2 Sla”, for 1-arm VAE (JointVAE) and 2-arm VAE (cpl-mixVAE). For each type, the traversal is color-mapped to a normalized reconstructed gene expression value (colorbar) as a function of the state variable for 3 gene subsets: marker genes (MG), immediate early genes (IEG), and housekeeping genes (HKG).

References

- Aitchison, J. The statistical analysis of compositional data. *Journal of the Royal Statistical Society: Series B (Methodological)*, 44(2):139–160, 1982.
- Andrews, T. S. and Hemberg, M. Identifying cell populations with scRNA-seq. *Molecular aspects of medicine*, 59: 114–122, 2018.
- Antoniou, A., Storkey, A., and Edwards, H. Data augmentation generative adversarial networks. *arXiv preprint arXiv:1711.04340*, 2017.
- Bargmann, C., Newsome, W., Anderson, A., Brown, E., Deisseroth, K., Donoghue, J., MacLeish, P., Marder, E., Normann, R., Sanes, J., et al. Brain 2025: a scientific vision. *Brain Research through Advancing Innovative Neurotechnologies (BRAIN) Working Group Report to the Advisory Committee to the Director, NIH*, 2014.
- Bengio, Y., Courville, A., and Vincent, P. Representation learning: A review and new perspectives. *IEEE transactions on pattern analysis and machine intelligence*, 35(8): 1798–1828, 2013.
- Blei, D. M., Kucukelbir, A., and McAuliffe, J. D. Variational inference: A review for statisticians. *Journal of the American statistical Association*, 112(518):859–877, 2017.
- Blum, A. and Mitchell, T. Combining labeled and unlabeled data with co-training. In *Proceedings of the eleventh annual conference on Computational learning theory*, pp. 92–100, 1998.
- Bouchacourt, D., Tomioka, R., and Nowozin, S. Multi-level variational autoencoder: Learning disentangled representations from grouped observations. *arXiv preprint arXiv:1705.08841*, 2017.
- Burgess, C. P., Higgins, I., Pal, A., Matthey, L., Watters, N., Desjardins, G., and Lerchner, A. Understanding disentangling in β -vae. *arXiv preprint arXiv:1804.03599*, 2018.
- Chen, X., Duan, Y., Houthoofd, R., Schulman, J., Sutskever, I., and Abbeel, P. Infogan: Interpretable representation learning by information maximizing generative adversarial nets. In *Advances in neural information processing systems*, pp. 2172–2180, 2016.
- Deasy, J., Simidjievski, N., and Liò, P. Constraining variational inference with geometric jensen-shannon divergence. *arXiv preprint arXiv:2006.10599*, 2020.
- Dilokthanakul, N., Mediano, P. A., Garnelo, M., Lee, M. C., Salimbeni, H., Arulkumaran, K., and Shanahan, M. Deep unsupervised clustering with gaussian mixture variational autoencoders. *arXiv preprint arXiv:1611.02648*, 2016.
- Dupont, E. Learning disentangled joint continuous and discrete representations. In *Advances in Neural Information Processing Systems*, pp. 710–720, 2018.
- Egozcue, J. J., Pawłowsky-Glahn, V., Mateu-Figueras, G., and Barcelo-Vidal, C. Isometric logratio transformations for compositional data analysis. *Mathematical Geology*, 35(3):279–300, 2003.
- Feng, F., Wang, X., and Li, R. Cross-modal retrieval with correspondence autoencoder. In *Proceedings of the 22nd ACM international conference on Multimedia*, pp. 7–16, 2014.
- Gala, R., Gouwens, N., Yao, Z., Budzillo, A., Penn, O., Tasic, B., Murphy, G., Zeng, H., and Sümbül, U. A coupled autoencoder approach for multi-modal analysis of cell types. In *Advances in Neural Information Processing Systems*, pp. 9263–9272, 2019.
- Guo, F., Wang, X., Fan, K., Broderick, T., and Dunson, D. B. Boosting variational inference. *arXiv preprint arXiv:1611.05559*, 2016.
- Higgins, I., Matthey, L., Pal, A., Burgess, C., Glorot, X., Botvinick, M., Mohamed, S., and Lerchner, A. beta-vae: Learning basic visual concepts with a constrained variational framework. *Iclr*, 2(5):6, 2017.
- Hosoya, H. Group-based learning of disentangled representations with generalizability for novel contents. In *IJCAI*, pp. 2506–2513, 2019.
- Hrvatin, S., Hochbaum, D. R., Nagy, M. A., Cicconet, M., Robertson, K., Cheadle, L., Zilionis, R., Ratner, A., Borges-Monroy, R., Klein, A. M., et al. Single-cell analysis of experience-dependent transcriptomic states in the mouse visual cortex. *Nature neuroscience*, 21(1):120–129, 2018.
- Jang, E., Gu, S., and Poole, B. Categorical reparameterization with gumbel-softmax. *arXiv preprint arXiv:1611.01144*, 2016.
- Jeong, Y. and Song, H. O. Learning discrete and continuous factors of data via alternating disentanglement. *arXiv preprint arXiv:1905.09432*, 2019.
- Jiang, Z., Zheng, Y., Tan, H., Tang, B., and Zhou, H. Variational deep embedding: an unsupervised and generative approach to clustering. In *Proceedings of the 26th International Joint Conference on Artificial Intelligence*, pp. 1965–1972, 2017.
- Johnson, M. J., Duvenaud, D. K., Wiltchko, A., Adams, R. P., and Datta, S. R. Composing graphical models with neural networks for structured representations and fast inference. In *Advances in neural information processing systems*, pp. 2946–2954, 2016.

- Kim, H. and Mnih, A. Disentangling by factorising. *arXiv preprint arXiv:1802.05983*, 2018.
- Kingma, D. P. and Welling, M. Auto-encoding variational bayes. *arXiv preprint arXiv:1312.6114*, 2013.
- Kingma, D. P., Salimans, T., Jozefowicz, R., Chen, X., Sutskever, I., and Welling, M. Improving variational inference with inverse autoregressive flow. *arXiv preprint arXiv:1606.04934*, 2016.
- Kumar, A. and Daumé, H. A co-training approach for multi-view spectral clustering. In *Proceedings of the 28th international conference on machine learning (ICML-11)*, pp. 393–400, 2011.
- Larsen, A. B. L., Sønderby, S. K., Larochelle, H., and Winther, O. Autoencoding beyond pixels using a learned similarity metric. In *International conference on machine learning*, pp. 1558–1566. PMLR, 2016.
- Lee, M. and Pavlovic, V. Private-shared disentangled multimodal vae for learning of hybrid latent representations. *arXiv preprint arXiv:2012.13024*, 2020.
- Locatello, F., Bauer, S., Lucic, M., Rätsch, G., Gelly, S., Schölkopf, B., and Bachem, O. Challenging common assumptions in the unsupervised learning of disentangled representations. *arXiv preprint arXiv:1811.12359*, 2018a.
- Locatello, F., Dresdner, G., Khanna, R., Valera, I., and Rätsch, G. Boosting black box variational inference. In *Advances in Neural Information Processing Systems*, pp. 3401–3411, 2018b.
- Locatello, F., Poole, B., Rätsch, G., Schölkopf, B., Bachem, O., and Tschannen, M. Weakly-supervised disentanglement without compromises. *arXiv preprint arXiv:2002.02886*, 2020.
- Lucas, J., Tucker, G., Grosse, R. B., and Norouzi, M. Don't blame the elbo! a linear vae perspective on posterior collapse. In *Advances in Neural Information Processing Systems*, pp. 9403–9413, 2019.
- Maddison, C. J., Tarlow, D., and Minka, T. A* sampling. In *Advances in Neural Information Processing Systems*, pp. 3086–3094, 2014.
- Minka, T. et al. Divergence measures and message passing. Technical report, Citeseer, 2005.
- Monti, S., Tamayo, P., Mesirov, J., and Golub, T. Consensus clustering: a resampling-based method for class discovery and visualization of gene expression microarray data. *Machine learning*, 52(1-2):91–118, 2003.
- Nemeth, J. Adversarial disentanglement with grouped observations. In *Proceedings of the AAAI Conference on Artificial Intelligence*, volume 34, pp. 10243–10250, 2020.
- Pereyra, G., Tucker, G., Chorowski, J., Kaiser, Ł., and Hinton, G. Regularizing neural networks by penalizing confident output distributions. *arXiv preprint arXiv:1701.06548*, 2017.
- Quiroz, M., Nott, D. J., and Kohn, R. Gaussian variational approximation for high-dimensional state space models. *arXiv preprint arXiv:1801.07873*, 2018.
- Ranganath, R., Tran, D., and Blei, D. Hierarchical variational models. In *International Conference on Machine Learning*, pp. 324–333. PMLR, 2016.
- Shu, R., Chen, Y., Kumar, A., Ermon, S., and Poole, B. Weakly supervised disentanglement with guarantees. *arXiv preprint arXiv:1910.09772*, 2019.
- Surowiecki, J. *The wisdom of crowds*. Anchor, 2005.
- Tarasenko, T. N., Pacheco, S. E., Koenig, M. K., Gomez-Rodriguez, J., Kapnick, S. M., Diaz, F., Zerfas, P. M., Barca, E., Sudderth, J., DeBerardinis, R. J., et al. Cytochrome c oxidase activity is a metabolic checkpoint that regulates cell fate decisions during t cell activation and differentiation. *Cell metabolism*, 25(6):1254–1268, 2017.
- Tasic, B., Yao, Z., Graybuck, L. T., Smith, K. A., Nguyen, T. N., Bertagnolli, D., Goldy, J., Garren, E., Economo, M. N., Viswanathan, S., et al. Shared and distinct transcriptomic cell types across neocortical areas. *Nature*, 563(7729):72–78, 2018.
- Tian, K., Zhou, S., and Guan, J. Deepcluster: A general clustering framework based on deep learning. In *Joint European Conference on Machine Learning and Knowledge Discovery in Databases*, pp. 809–825. Springer, 2017.
- Trapnell, C. Defining cell types and states with single-cell genomics. *Genome research*, 25(10):1491–1498, 2015.
- Tschannen, M., Bachem, O., and Lucic, M. Recent advances in autoencoder-based representation learning. *arXiv preprint arXiv:1812.05069*, 2018.
- Zhang, C., Bütepage, J., Kjellström, H., and Mandt, S. Advances in variational inference. *IEEE transactions on pattern analysis and machine intelligence*, 41(8):2008–2026, 2018.